

## Original Articles

## Using the diurnal variation characteristics of effective quantum yield of PSII photochemistry for drought stress detection in maize

Zhuang Chen<sup>a,b</sup>, Zhigang Liu<sup>a,b,\*</sup>, Shuai Han<sup>a,b</sup>, Hao Jiang<sup>a,b</sup>, Shan Xu<sup>a,b,c</sup>, Huarong Zhao<sup>d,e</sup>, Sanxue Ren<sup>d,e</sup><sup>a</sup> State Key Laboratory of Remote Sensing Science, Jointly Sponsored by Beijing Normal University and Aerospace Information Research Institute of Chinese Academy of Sciences, Beijing 100875, China<sup>b</sup> Beijing Engineering Research Center for Global Land Remote Sensing Products, Institute of Remote Sensing Science and Engineering, Faculty of Geographical Science, Beijing Normal University, Beijing 100875, China<sup>c</sup> Plant Phenomics Research Centre, Academy for Advanced Interdisciplinary Studies, Nanjing Agricultural University, Nanjing 210095, China<sup>d</sup> Chinese Academy of Meteorological Sciences, Beijing 100081, China<sup>e</sup> Hebei Gucheng Agricultural Meteorology National Observation and Research Station, Baoding 072656, China

## ARTICLE INFO

## Keywords:

Effective quantum yield of PSII photochemistry  
 Photosynthetically active radiation  
 Diurnal variation  
 Drought stress

## ABSTRACT

The importance of detecting drought stress in crops to alleviate the pressure of the growing population and food demand is well recognized. Although chlorophyll fluorescence (ChlF) is closely related to photosynthesis, it is always disturbed by the intensity of irradiance during the measurement. To detect drought stress more effectively with ChlF, we studied the diurnal relationship of the effective quantum yield of photosystem II (PSII) photochemistry ( $\Phi_{PSII}$ ) and photosynthetically active radiation (PAR). We measured the diurnal  $\Phi_{PSII}$ , leaf temperature ( $T_{leaf}$ ) and PAR of maize leaves (*Zheng Dan 958*) by pulse-amplitude modulated (PAM) fluorometry under different drought stresses. We found that in the absence of drought stress, the linearity (indicated by  $R^2$ ) between diurnal  $\Phi_{PSII}$  and PAR was strong. When drought stress was gradually aggravated, the difference between the  $\Phi_{PSII}$  values in the morning and those in the afternoon under similar PAR values gradually became significant. Therefore, the  $R^2$  values of the linear correlation of the diurnal  $\Phi_{PSII}$ -PAR regression gradually decreased under increased drought stress. The simulation results of a photosynthesis model showed that the diurnal variation in the response of  $\Phi_{PSII}$ -PAR during drought may be the result of the fluctuation of the substrate saturated Rubisco capacity ( $V_{cmax}$ ), which was dominated by the dynamics of  $T_{leaf}$ . The results indicated that the linearity of diurnal  $\Phi_{PSII}$ -PAR regression can be used as an effective and convenient field indicator to monitor drought stress.

## 1. Introduction

Water limitation is considered the main factor, either alone or combined with other unfavourable conditions, that seriously limits agricultural productivity around the world (Trenberth et al., 2014). In the context of global climate changes, warmer and drier conditions are expected to be more frequent, leading to severe droughts. In addition, the contradiction between population pressure and food demand in the future will aggravate the impact of drought stress on the economy, geopolitics and society (Somerville et al., 2001; Tombesi et al., 2018). Therefore, it is particularly important to detect the physiological state of vegetation and study how vegetation responds to drought stress, which

helps to optimize the agricultural water demand and minimize the physiological damage and yield loss of crops.

During photosynthesis, ~5% of the light energy absorbed by photosystem II (PSII) is re-emitted as chlorophyll fluorescence (ChlF). ChlF is closely related to photosynthetic CO<sub>2</sub> assimilation. Therefore, ChlF can be used to monitor the responses of vegetation to various stresses, including drought stress (Percival, 2005; Salvatori et al., 2014). Although there are various fluorescence measurement techniques, the pulse-amplitude modulated (PAM) technique (Schreiber et al., 1987) is widely adopted because it is feasible for field applications (Brestic and Zivcak, 2013). PAM fluorometry has become a powerful tool in the research of plant photosynthesis and is increasingly being used for in situ

\* Corresponding author at: State Key Laboratory of Remote Sensing Science, Jointly Sponsored by Beijing Normal University and Aerospace Information Research Institute of Chinese Academy of Sciences, Beijing 100875, China.

E-mail address: [zhigangliu@bnu.edu.cn](mailto:zhigangliu@bnu.edu.cn) (Z. Liu).

<https://doi.org/10.1016/j.ecolind.2022.108842>

Received 9 February 2022; Received in revised form 31 March 2022; Accepted 3 April 2022

Available online 8 April 2022

1470-160X/© 2022 The Author(s). Published by Elsevier Ltd. This is an open access article under the CC BY-NC-ND license (<http://creativecommons.org/licenses/by-nc-nd/4.0/>).

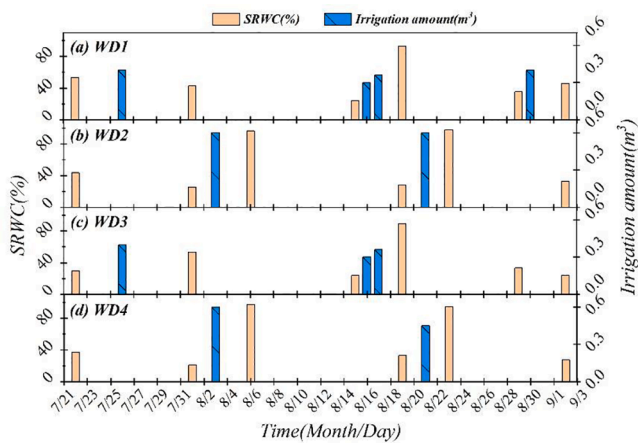


**Fig. 1.** The soil relative water content (SRWC) values and irrigation amounts of each plot from July 22 to September 2. The experimental rewatering time was the evening after the experimental observations of that day.

ecological monitoring (Campbell et al., 2003; Durako, 2012). The most widely used parameters include the maximum quantum yield of PSII photochemistry ( $\Phi_{PSII}^{max}$ ) and the effective quantum yield of PSII photochemistry ( $\Phi_{PSII}$ ).  $\Phi_{PSII}^{max}$  reflects the potential quantum efficiency of PSII, which is considered to be a susceptible component of the photosynthetic machinery and will often bear the brunt of stress conditions (Demmig-Adams and Adams, 2018). During severe drought,  $\Phi_{PSII}^{max}$  will decrease (Li et al., 2008; Brestic and Zivcak, 2013; Tribulato et al., 2019), indicating the downregulation of photosynthesis or photoinhibition under stress (Lichtenthaler and Rinderle, 1988). However, during mild to moderate drought stress,  $\Phi_{PSII}^{max}$  usually does not change obviously (Baker and Rosenqvist, 2004; Brestic and Zivcak, 2013). In addition, because dark adaptation is required, it is inconvenient to measure  $\Phi_{PSII}^{max}$  during the daytime in the field (Zha et al., 2017).  $\Phi_{PSII}$  reflects the actual efficiency of photosystem II (PSII) at a specific moment (Maxwell and Johnson, 2000; Baker, 2008). The measurement of  $\Phi_{PSII}$  does not require dark adaptation, which is convenient for field measurements (Brestic and Zivcak, 2013).  $\Phi_{PSII}$  is extremely sensitive to changes of environmental factors, such as the soil moisture and light conditions (O'Neill et al., 2006; Murchie and Lawson, 2013; Hazrati et al., 2016; Lang et al., 2018). For drought stress detection in the field, it is difficult to decouple the contributions of drought stress and high irradiance to the decrease in

$\Phi_{PSII}$ . Therefore, it is difficult to determine the degree of drought stress based on only absolute  $\Phi_{PSII}$  values.

To better exploit the potential of PAM technology in plant physiological detection, many studies have attempted to improve the measurement scheme for obtaining fluorescence parameters. The rapid light curve (RLC) method measures  $\Phi_{PSII}$  as a function of irradiance (White and Critchley, 1999). Through RLC, a series of parameters for analysing vegetation physiology can be derived. For example, the initial slope and the asymptote of the RLC are measures of the light harvesting efficiency of photosynthesis and the capacity of photosystems, respectively (Marshall et al., 2000). RLC has been applied in detecting drought stress (Huang et al., 2012) and high-temperature stress of plants (Datko et al.

**Table 1**

Input parameter setting of the biochemical module in SCOPE.

Parameter	Values	Units	Description
$V_{cmax,25}$	40	$\mu\text{mol}\cdot\text{m}^{-2}\cdot\text{s}^{-1}$	maximum carboxylation capacity @ 25°C
$T_{leaf}$	30,35,40,45,50	°C	leaf temperature
Type	C4	-	C4 plant
$PAR_{leaf}$	0-1500	$\mu\text{mol}\cdot\text{photons}\cdot\text{m}^{-2}\cdot\text{s}^{-1}$	net radiation, PAR

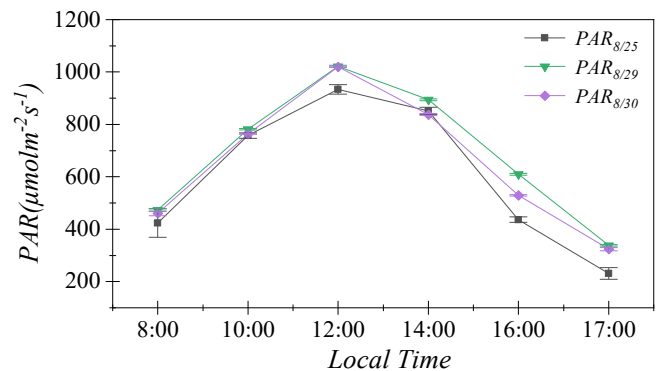


**Fig. 3.** The diurnal variations of the PAR received by leaves that were levelled. The error bars represent the variances of the measured results at that time.

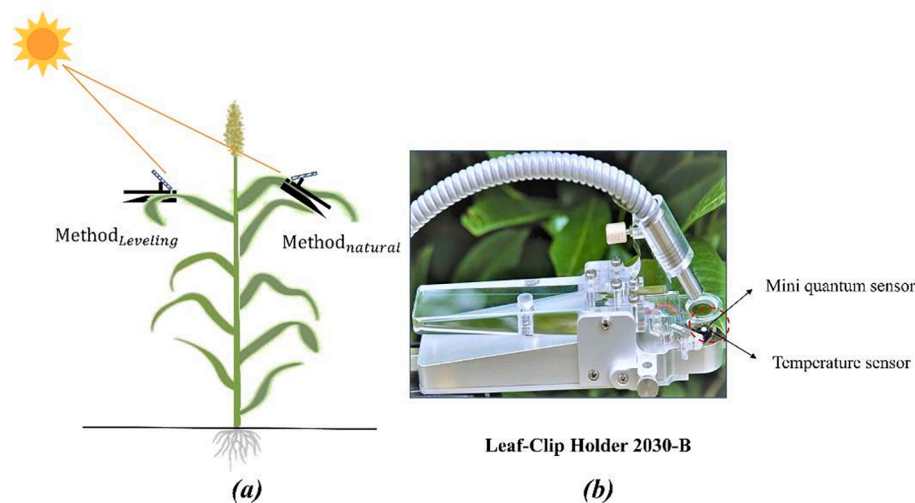


**Fig. 2.** Two methods of  $\Phi_{PSII}$  measurement. The Leaf-Clip Holder 2030-B was equipped with a Mini quantum sensor and a temperature sensor (b). A mini quantum sensor was integrated into the Leaf-Clip Holder to monitor the PAR to which samples were exposed. A Ni-CrNi thermocouple was attached to the lower part of the leaf clip, and its probe was gently placed against the lower surface of the leaf to determine its temperature.

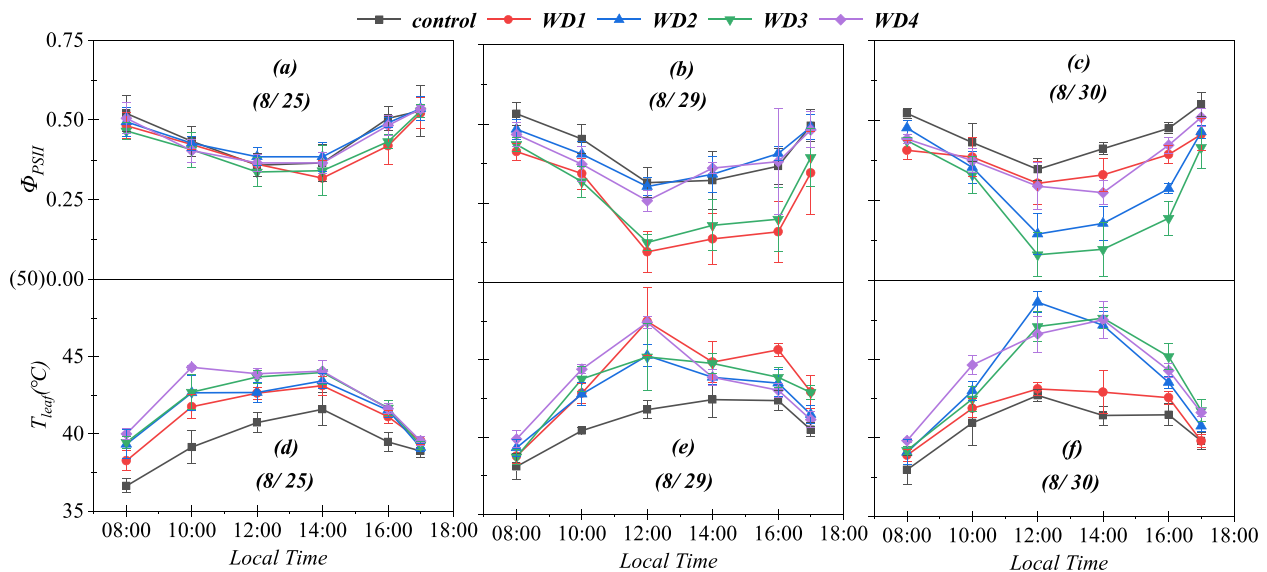


**Fig. 4.** Diurnal variations of the  $\Phi_{PSII}$  and  $T_{Leaf}$  values of the control, WD1, WD2, WD3, and WD4 treatments from August 25 to August 30. The error bars represent the variances of the measured results at that time.

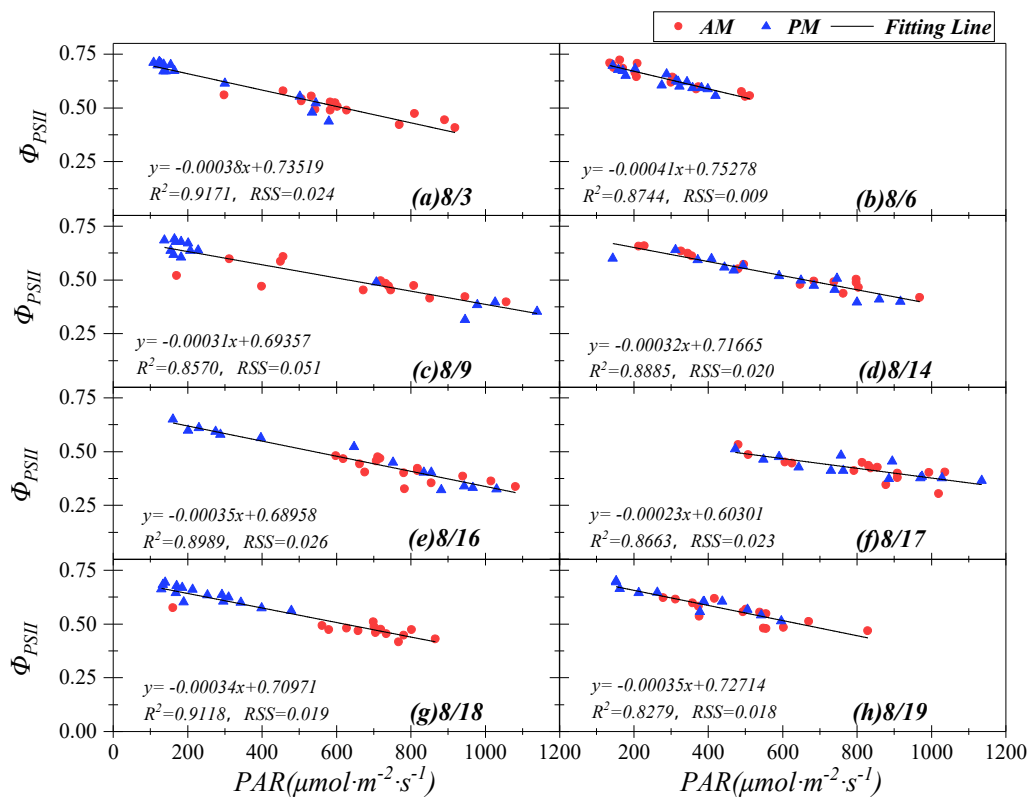


**Fig. 5.**  $\Phi_{PSII}$  versus irradiance at the leaf of maize measured during the days of August 3 to August 19 in the control plot. The red dots represent the data measured in the morning, and the blue triangles represents the data measured in the afternoon. The solid lines represent the fitted regression equations. RSS represents the root mean square error of the regression equation.

2008). However, RLC still only reflects the photosynthetic physiological state of plants at a specific time of day (Belshe et al., 2007). In addition, a clip is required to exclude ambient light from the sample during the measurement of RLC. Thus, it is difficult to measure RLC curves automatically throughout the day. To strip out the influence of irradiance intensity on  $\Phi_{PSII}$  in monitoring the physiological condition of plants, Durako. (2012) suggested obtaining PAM-fluorescence over diurnal periods and using the regression slope and y-intercept of  $\Phi_{PSII}$  versus

PAR, rather than absolute  $\Phi_{PSII}$  values, to detect responses of plants to stresses. The experimental results of Howarth and Durako (2013) and Zha et al. (2017) confirmed that the y-intercept of diurnal  $\Phi_{PSII}$ -PAR regression can serve as a good proxy for  $F_v/F_m$  to assess the physiological status of plants. These studies indicate that the regression of diurnal  $\Phi_{PSII}$ -PAR is a promising method of physiological assessment with the ChlF technique.

However, the effectiveness of the diurnal  $\Phi_{PSII}$ -PAR regression

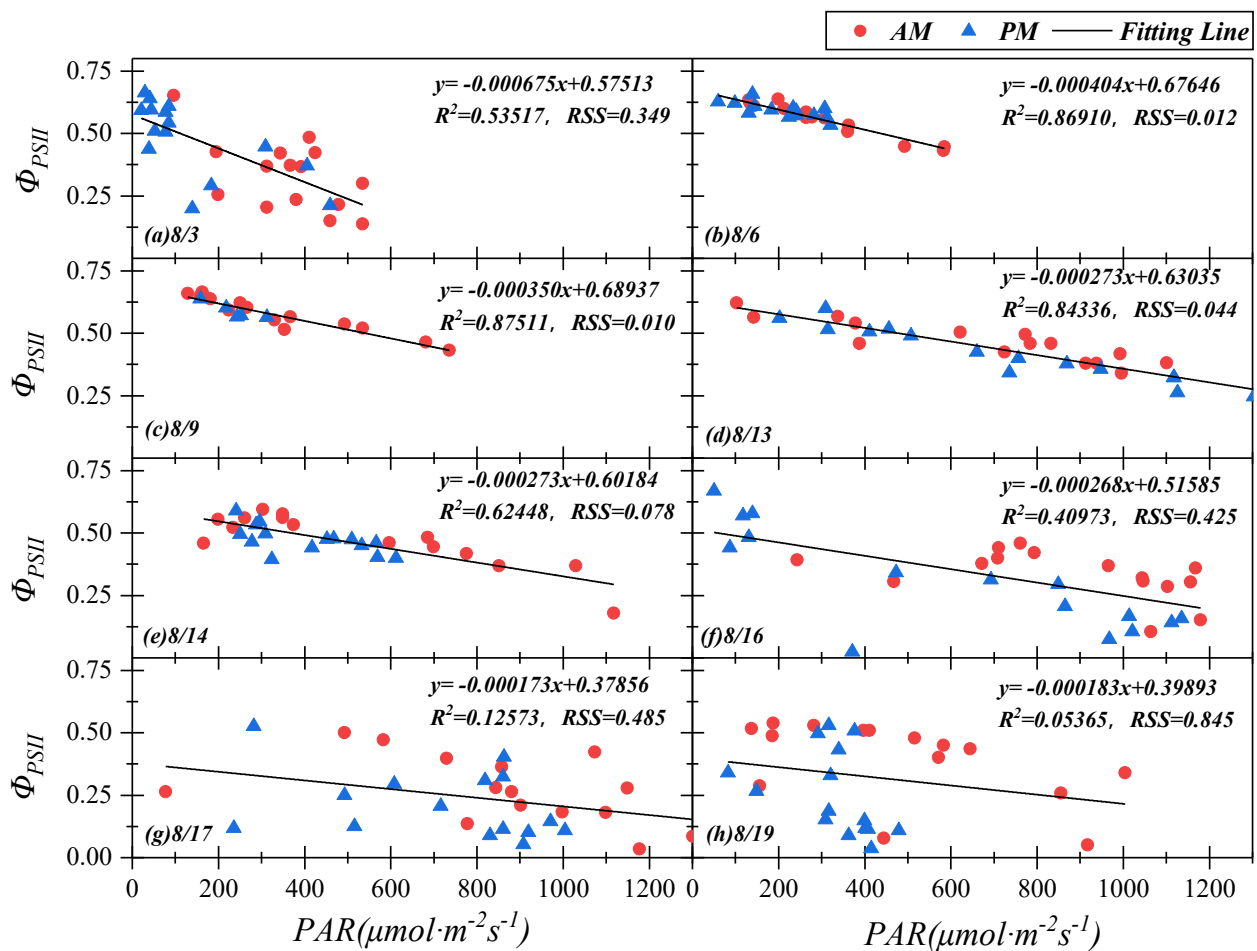


Fig. 6.  $\Phi_{PSII}$  versus irradiance of the leaf of maize measured during the days of August 3 to August 19 in WD4. The red dots represent the data measured in the morning, and the blue triangles represent the data measured in the afternoon. The solid lines represent the fitted regression equations.

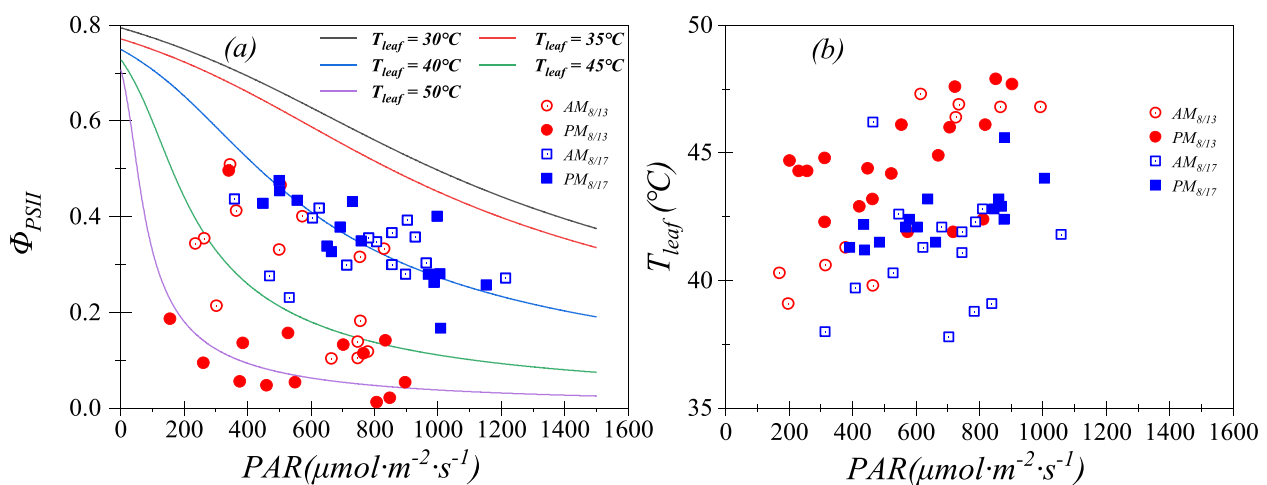


Fig. 7. The red dots and blue squares represent  $\Phi_{PSII}$  (a)  $T_{leaf}$  (b) of the WD3 plot on August 13 and August 17, respectively. The hollow dots and the solid dots represent the morning (8:00–12:00 local time) and afternoon (13:00–17:00 local time) data, respectively. It should be noted that plot WD3 was under drought stress on August 13, while there was no drought stress on August 17. The solid curve in (a) is the variation of  $\Phi_{PSII}$  obtained through the simulation of the biochemical module in the SCOPE.

method in assessing drought stress remains to be evaluated. To study the diurnal response of  $\Phi_{PSII}$  to PAR under different drought stresses, we measured diurnal  $\Phi_{PSII}$  and PAR in maize leaves in a field experiment under water control. Additionally, we simulated the variations of  $\Phi_{PSII}$

with different light intensities with a photosynthesis model (Van der Tol et al., 2014). The specific objectives of our study were to (1) explore the diurnal variations of the response of  $\Phi_{PSII}$  to PAR under different degrees of drought stress and (2) evaluate the effectiveness of the different

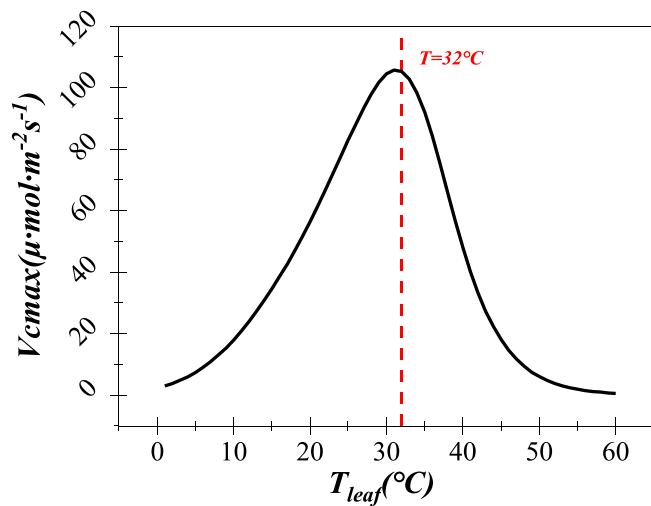


Fig. 8. Relationship between  $T_{leaf}$  and  $V_{cmax}$  simulated by the photosynthesis model in SCOPE.

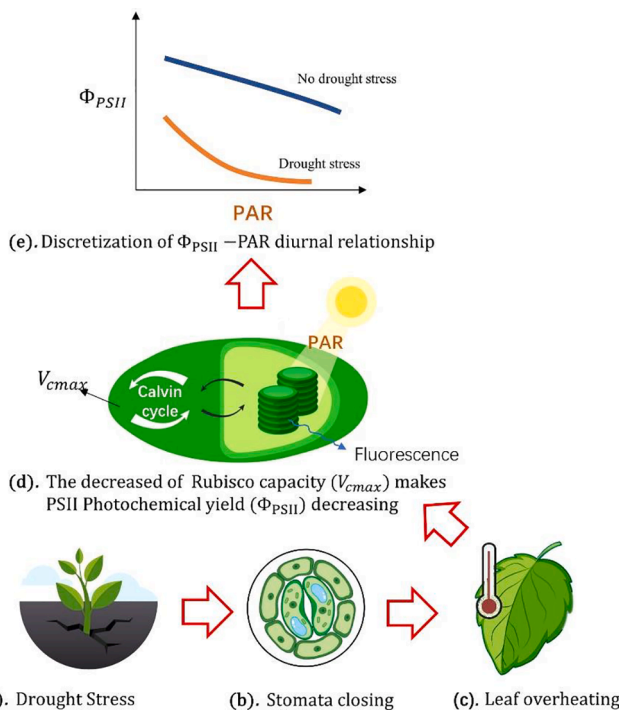


Fig. 9. The possible responses of plant photosynthesis to drought stress. Drought stress caused stomatal closure in leaves (a-b). The closure of the stomata led to excessive  $T_{leaf}$  values (b-c). Excessive  $T_{leaf}$  values caused the substrate saturated Rubisco capacity ( $V_{cmax}$ ) to decrease, and the decreases of  $V_{cmax}$  decreased  $\Phi_{PSII}$  (c-d). The linear relationship of  $\Phi_{PSII}$ -PAR weakened (e).

diurnal  $\Phi_{PSII}$ -PAR regression parameters, including slopes, y-intercepts and coefficients of determination ( $R^2$ ), to monitor drought stress.

## 2. Materials and methods

### 2.1. Experimental scheme

The study area was located at the Gucheng Meteorological Science Research Station, Dingxing County, Baoding City, China (115°44'36"E, 39°9'26"N). Maize (*Zheng Dan 958*) was planted in five 2 × 4 m plots, which were isolated from each other and the surrounding soil by

concrete walls to avoid the exchange of soil moisture. A movable rain shelter was placed over these plots to protect against rainfall. In this experiment, the maize was sown on June 21, 2019. During the growth of maize, the soil moisture of each plot was controlled by artificial irrigation. There were no significant differences in water content among the plots during the period from the sowing stage to the growing stage. After July 26, we imposed different water deficits on these plots (named control, WD1, WD2, WD3, WD4). The soil relative water content (SRWC) values and irrigation amounts of each plot are listed in Fig. 1. Among them, only the maize in the control plot received an adequate water supply throughout the growing season. Thus, the SRWCs and irrigation amounts of the control plot were not recorded and are not shown in Fig. 1.

The SRWC values were measured before and after each irrigation to evaluate the degree of water stress from July 21 to September 2. Soil samples were collected at depths of 5 cm, 10 cm, and 20 cm. Within 10 min after the soil samples were obtained, we weighed the soil samples and determined the weight of the wet soil ( $W_{wet}$ ). We then put the soil samples in an oven at 105 °C and dried for 24 h. After ensuring that all water had been completely removed from the soil samples, we weighed the dried samples again to obtain the weight of the dry soil ( $W_{dry}$ ). The SRWC values were calculated using the ratio of the weight moisture capacity (WMC) and field water-holding capacity (WHC) of the soil according to the drying method (O'Kelly, 2004):

$$SRWC = WMC/WHC \times 100\% \quad (1)$$

The value of the optimum WHC was set at 22.7 according to previous research (Zhao et al., 2018). The WMC of each soil sample was calculated by:

$$WMC = (W_{wet} - W_{dry})/W_{wet} \quad (2)$$

The averages of the SRWCs at the 0 ~ 20 cm depths were used in this study (Fig. 1).

### 2.2. Measurement parameters

The diurnal variations in  $\Phi_{PSII}$ , leaf temperature ( $T_{leaf}$ ) and PAR of the leaves sampled under different water conditions were measured synchronously with a portable PAM fluorometer (PAM-2500, Walz, Effeltrich, Germany) every two hours beginning at 8:00 am and ending at 18:00 pm. During each measurement, 5 ~ 7 blades were randomly selected from each plot. The  $T_{leaf}$  and PAR of each sampled leaf were measured by a Ni-CrNi thermocouple and a micro photon probe on the Leaf-Clip Holder 2030-B of the PAM fluorometer (Fig. 2b), respectively.

To avoid the influence of shadows, we only sampled the leaves in the upper layer of the canopy. Two methods were adopted to measure leaf parameters (Fig. 2a). One method maintained the natural attitude of the leaf during measurements (Method<sub>natural</sub>) during the period of August 3 to August 19. Due to differences of orientation, the PAR values of each sampled leaf measured by Method<sub>natural</sub> could vary significantly. The other method levelled the leaf upwards during measurements (Method<sub>leveling</sub>) during the period of August 25 to August 30. In addition, considering the variations of the incident irradiance during the measurement of each group, we fine-tuned the angle of the leaves to ensure that the PAR values of each leaf in a group were close to each other. Measurement values were recorded after the fluorescence signals stabilized.

$\Phi_{PSII}$  was calculated according to (Genty et al. 1989) by the equation shown below:

$$\Phi_{PSII} = (F'_m - F_t) / F'_m \quad (3)$$

where  $F'_m$  is the light-adapted maximum fluorescence,  $F_t$  is the steady-state chlorophyll fluorescence.

### 2.3. Simulation of $\Phi_{PSII}$

In this research, the SCOPE 2.0 (Soil Canopy Observation of Photosynthesis and Energy fluxes) model (Yang et al., 2021; Van der Tol et al., 2009), including a biochemical module that combines the photosynthesis model with the fluorescence model, was used to simulate the variations of  $\Phi_{PSII}$  with light intensity. In the biochemical module, the values of  $\Phi_{PSII}$  for C4 crops can be calculated through the fraction of absorbed photosynthetically active radiation ( $fPAR$ ) and the gross assimilation rate ( $A$ ), which is the minimum of three potential capacities: the light-limited assimilation rate ( $A_E$ ), the Rubisco-limited rate ( $A_C$ ), and the rate imposed by sucrose synthesis ( $A_S$ ) (Collatz et al., 1991; Collatz et al., 1992). The details of the specific calculations can be found in (Van der Tol et al., 2014). In the calculation of  $A_C$ , substrate saturated Rubisco capacity ( $V_{cmax}$ ) is the key parameter. Under natural conditions, the influence of  $V_{cmax}$  depends mainly on chlorophyll content and  $T_{leaf}$  (Grassi et al. 2005). Since the diurnal variation of chlorophyll content is usually relatively small, it can be ignored. Therefore, in this study, we only simulated the change of  $V_{cmax}$  with  $T_{leaf}$  using the following formula (Collatz et al., 1992; Porcar-Castell et al., 2014):

$$V_{cmax} = \frac{\exp[0.0742(T_{leaf} - 25)]}{(1 + \exp[0.3(T_{leaf} - 35)])(1 + \exp[0.2(8 - T_{leaf})])} V_{cmax,25} \quad (4)$$

where  $V_{cmax,25}$  is the maximum carboxylation capacity at 25°C. For unstressed leaves of maize,  $V_{cmax,25}$  was approximately  $40 \mu\text{mol}\cdot\text{m}^{-2}\cdot\text{s}^{-1}$  (Collatz et al., 1992). In this study, the parameter  $V_{cmax,25}$  of maize in the growth stage was not obtained, and  $40 \mu\text{mol}\cdot\text{m}^{-2}\cdot\text{s}^{-1}$  was used in the simulation. Generally,  $fPAR$  of leaves is in the range of 0.8 to 0.9 (Pearcy and Yang, 1996). In SCOPE 2.0, the default setting for  $fPAR$  was 0.83, so we used that value. The settings of the other parameters in the simulation are shown in Table 1.

### 2.4. Data processing and statistical analysis

Raw data were processed using the PamWin-3 software (<https://www.walz.com/>). Values of  $\Phi_{PSII}$  under 0 (nondimensional) were considered abnormal and were removed from the dataset. The scatter plots of  $\Phi_{PSII}$  with PAR during the day were fitted based on the following formula (Durako, 2012; Howarth and Durako, 2013):

$$\Phi_{PSII} = a \times PAR + b \quad (5)$$

The diurnal data points in the regression ranged from August 3 to August 19. The regression slopes and y-intercepts of the diurnal  $\Phi_{PSII}$ -PAR relationship were used to examine the diurnal physiological variations of maize in response to changes in soil moisture conditions.

Meanwhile, the coefficient of determination ( $R^2$ ) values were calculated using Equation (6):

$$R^2 = 1 - \frac{\sum_{i=1}^n (y_i - \hat{y}_i)^2}{\sum_{i=1}^n (y_i - \bar{y})^2} \quad (6)$$

where  $n$  represents the number of leaves sampled in each plot in a day.  $\bar{y}$  denotes the average of the observations and  $\hat{y}_i$  is the prediction of  $y_i$  using the fitted model in Equation (6).

## 3. Results

### 3.1. Diurnal variations of $\Phi_{PSII}$ obtained through *Method<sub>levelling</sub>*

In the *Method<sub>levelling</sub>* experiments, because the incoming irradiances of leaves from all plots at each sample time were approximately equal, the anomalies of  $\Phi_{PSII}$  and  $T_{leaf}$  caused by drought stress could be directly shown by their diurnal variation curves. Because the sky was clear during the experiments, the diurnal variation curves of the irradiance intensity were close to a symmetrical cosine curve (Fig. 3). Accordingly,

the diurnal variation curves of  $\Phi_{PSII}$  and  $T_{leaf}$  of the leaves under no water stress were approximately concave and convex symmetrical curves, respectively (Fig. 4a, d). However, under drought stress, the diurnal variation curves of  $\Phi_{PSII}$  and  $T_{leaf}$  became asymmetrical (Fig. 4c, f). In the morning, the values of  $\Phi_{PSII}$  and  $T_{leaf}$  of the different water-treated plots were similar. However, at noon and in the early afternoon, under drought stress, the  $\Phi_{PSII}$  values became significantly smaller than those not under stress. And the  $T_{leaf}$  values became significantly higher than those not under stress. After rewetting, the curve shapes and the magnitudes of the diurnal  $\Phi_{PSII}$  and  $T_{leaf}$  values of plot WD1 recovered (Fig. 4c, f).

### 3.2. Diurnal variations of $\Phi_{PSII}$ obtained through *Method<sub>natural</sub>*

During the period of August 3 to 19, the diurnal variations of  $\Phi_{PSII}$  were obtained using *Method<sub>natural</sub>*. In contrast to the results of *Method<sub>levelling</sub>*, although the light intensity changed little during each sampling time, the PAR values measured from each sampled leaf were significantly different because of the different leaf postures. Therefore, the diurnal curves of  $\Phi_{PSII}$  measured by the *Method<sub>natural</sub>* fluctuated in an irregular manner. Nevertheless, we found differences caused by drought stress through the scatter plot of  $\Phi_{PSII}$  with PAR (Figs. 5, 6).

Under no water stress, the diurnal  $\Phi_{PSII}$  and PAR characteristics of the control plot were negatively linearly correlated with high significance (Fig. 5). The  $R^2$  values ranged from 0.83 to 0.92 (Fig. 5; Fig. A1-a). The regression y-intercepts and slopes were also stable at approximately 0.7 and  $-3.36 \times 10^{-4}$ , respectively (Fig. 5; Fig. A2-a). In addition, when the irradiance intensities were similar, the  $\Phi_{PSII}$  values in the morning (8:00–12:00 local time) were similar to those in the afternoon (13:00–17:00 local time).

As drought stress increased, the significance of the linear correlation between diurnal  $\Phi_{PSII}$ -PAR gradually weakened. For example, after irrigation in the evening (21:00 local time) of August 3, the  $R^2$  of the diurnal  $\Phi_{PSII}$ -PAR regressions of the WD4 plot increased from 0.54 on August 3 to 0.87 on August 6 (Fig. 6a, b). During the period of August 9 to August 13, the values of the y-intercepts, slopes and  $R^2$  remained stable and were similar to those of the well-watered control plot (Fig. 6b, c, d). Then, with the aggravation of the drought stress, the slopes and y-intercepts gradually decreased. In addition, the  $\Phi_{PSII}$  values in the morning (8:00–12:00 local time) were obviously larger than those in the afternoon (13:00–17:00 local time) under similar irradiance. Thus, the  $R^2$  values sharply decreased from the maximum value of 0.88 to the minimum value of 0.05 (Fig. 6c-h). The results of the WD1, WD2 and WD3 plots were similar to those of the WD4 plot (Figs. A1, A2). Meanwhile, we examined the relationship between the linear regression coefficients ( $R^2$ , slope and y-intercept) of diurnal  $\Phi_{PSII}$ -PAR regression and SRWC (Fig. A3). Compared with slope and y-intercept,  $R^2$  of diurnal  $\Phi_{PSII}$ -PAR regression had a stronger linear correlation with SRWC ( $R^2 = 0.98$ ,  $p < 0.05$ ).

### 3.3. Simulation of $\Phi_{PSII}$

The simulation results of the photosynthesis model show that the shape of the response curves of  $\Phi_{PSII}$  to PAR varied significantly with  $T_{leaf}$  (Fig. 7a). When  $T_{leaf}$  was approximately 32 °C, the value of  $V_{cmax}$  was the highest (Fig. 8), and the value of  $\Phi_{PSII}$  decreased at an approximately constant slope as the PAR increased. Therefore,  $\Phi_{PSII}$  and PAR were approximately linearly related under this condition (Fig. 7a). However, if the leaf temperature exceeded the optimum temperature,  $V_{cmax}$  decreased rapidly (Fig. 8). This led to two results: 1) The irradiance intensity at the transition point from the light-limiting stage to the Rubisco-limiting stage decreased (Fig. A4); 2) The  $\Phi_{PSII}$ -PAR curve of the Rubisco limiting stage, in which the gross assimilation increased at a slow rate or remained constant, became a reciprocal function curve with first a rapid decline and then a slow decline. Therefore, when  $T_{leaf}$  was

higher than 35 °C, the curvature of the  $\Phi_{PSII}$ -PAR curves increased, and the linear correlation between  $\Phi_{PSII}$  and PAR gradually weakened (Fig. 7a).

To analyze the relationship between the diurnal  $\Phi_{PSII}$ -PAR pattern and  $T_{leaf}$ , the morning and afternoon measurements of  $\Phi_{PSII}$ , PAR and  $T_{leaf}$  in the WD3 plot under different drought stresses are compared in Fig. 7. During the drought (August 13) stress, the morning points and the afternoon points are separated markedly in the  $\Phi_{PSII}$ -PAR scatter plot. The morning points were concentrated between the simulated curves of 40 °C and 45 °C, while the afternoon points were concentrated below the simulated curve of 45 °C. Correspondingly, the  $T_{leaf}$  measured in the morning was generally lower than that in the afternoon. After rehydration (August 17), the morning points and afternoon points in the scatter plot of  $\Phi_{PSII}$ -PAR were mainly concentrated around the simulated curve of 40 °C, with no significant differences. At this time, there were no significant differences between the measured  $T_{leaf}$  in the morning and afternoon, and most of them remained below 42.5 °C. Therefore, both the measured data and simulation results indicated that  $T_{leaf}$  played an important role in regulating the response of  $\Phi_{PSII}$  to PAR.

## 4. Discussion

### 4.1. Diurnal linearity of the $\Phi_{PSII}$ -PAR

To solve the problem that  $\Phi_{PSII}$  is sensitive to specific irradiance conditions during sampling, Durako (2012) proposed the  $\Phi_{PSII}$ -PAR regression approach to integrating the diurnal variations of light into physiological analysis and suggested using the intercepts and slopes of the regression as indicators to evaluate the health of the vegetation. The feasibility of this method in detecting maize drought was investigated in this study. Our results show that the diurnal variations of plant physiology under drought stress will inevitably induce the weakening of the linear correlation of diurnal  $\Phi_{PSII}$ -PAR. Therefore, we propose that the significance of the linear correlation can be used as a more reliable indicator for drought evaluation.

Our experimental and simulation results show that under conditions of sufficient water, there was a strong negative linear correlation between the diurnal  $\Phi_{PSII}$  and PAR. The correlation was obvious in the scatter plot  $\Phi_{PSII}$  and PAR obtained by Method<sub>natural</sub> (Fig. 5). Regarding the results of Method<sub>levelling</sub>, this correlation represents the symmetry of the diurnal  $\Phi_{PSII}$  curves when the sky was clear (Fig. 4a). The simulation results of the photosynthesis model show that when leaf temperature was suitable, the relationship between  $\Phi_{PSII}$  and PAR had an approximately linear negative correlation (Fig. 7a). Without drought stress, transpiration with high stomatal conductance can keep the leaf temperature in a suitable range (Flexas et al., 2004; Grassi et al., 2005; Koerber et al., 2012), which was confirmed by our experimental data (Fig. 4d, e, f; Fig. 7b). Thus, the simulation results also indirectly indicate that, when not under drought stress, the diurnal  $\Phi_{PSII}$  and PAR values will be approximately linearly correlated.

When drought stress occurred, the linear relationship of  $\Phi_{PSII}$ -PAR weakened. The scatter plot of  $\Phi_{PSII}$ -PAR obtained by Method<sub>natural</sub> became discrete, and the linear correlations of diurnal  $\Phi_{PSII}$ -PAR regressions became low (Fig. 6g, h). In the result of Method<sub>levelling</sub>, the diurnal variation curves of  $\Phi_{PSII}$  became asymmetrical even though the diurnal variation curves of PAR were symmetrical (Fig. 4b), which indicated that the correlations of the diurnal  $\Phi_{PSII}$ -PAR regressions decreased. The results simulated by the photosynthesis model show that under drought stress, the decrease in the linear correlation of diurnal  $\Phi_{PSII}$ -PAR regressions may be caused mainly by the following two reasons. 1) under drought stress conditions, closing of the stomata reduces evaporative cooling (Pallas et al., 1967; Kirschbaum, 1988; Fig. 9a, b) and  $T_{leaf}$  increases (Fig. 4d, e, f; Fig. 9c). Excessive  $T_{leaf}$  not only caused  $V_{cmax}$  to sharply decrease (Fig. 9d) but it also decreased the transition point between the light limitation state and the Rubisco saturation

limitation state (Vongcharoen et al., 2019; Fig. 3b). Thus, under a high  $T_{leaf}$ , the  $\Phi_{PSII}$ -PAR relationship changed from linear to nonlinear (Fig. 7a). 2) Under drought stress, the differences of  $T_{leaf}$  increased during the daytime. In the morning, the differences of  $T_{leaf}$  between drought stress and no drought stress were small. These differences increased gradually and peaked at noon and in the early afternoon (Fig. 4f). It should be noted that stomatal closure due to water stress will not only increase  $T_{leaf}$  but also decrease the availability of CO<sub>2</sub>. Both are likely to impinge on photosynthetic CO<sub>2</sub> fixation and reduce  $\Phi_{PSII}$ . However, because the CO<sub>2</sub>-concentrating mechanism is capable of saturating C4 photosynthesis under relatively low intercellular CO<sub>2</sub> concentrations (Ghannoum 2009), CO<sub>2</sub> availability tends to have a smaller effect on the photosynthetic rate of C4 plants (such as maize) than temperature (Lal and Edwards, 1996). This may be the reason why the measured values of  $\Phi_{PSII}$  at noon and early afternoon during water stress were just slightly lower than the simulated values considering only the  $T_{leaf}$  (Fig. 7).

The differences of  $T_{leaf}$  in a day may be caused by the light history (Müller et al., 2001), the diurnal variations of the soil water supply capacity and the leaf water potential (Oliver et al., 2010). Therefore, in the morning, the values of  $\Phi_{PSII}$  were high and were approximately linearly negatively correlated with PAR. At noon and in the early afternoon, the values of  $\Phi_{PSII}$  significantly decreased and became non-linearly related to PAR (Fig. 9e, f). With the aggravation of drought stress, the scatter plots of diurnal  $\Phi_{PSII}$ -PAR became increasingly more discrete (Fig. 6e, f, g, h).

### 4.2. Drought stress detection

Based on the  $\Phi_{PSII}$ -PAR regression approach, Durako (2012) proposed using the slopes and y-intercepts of the regressions as physiological indicators. The experiments on a desert shrub species verified the high correlations between the y-intercepts of the diurnal  $\Phi_{PSII}$ -PAR regressions and  $F_v/F_m$  on a diurnal scale (Zha et al. 2017). Our results show that the y-intercepts and slopes could reflect the evolution of drought on a diurnal scale in many cases (Fig. 7) because drought stress caused the values of  $\Phi_{PSII}$  to decrease and become less sensitive to high irradiance. However, the application of the y-intercept and slope will not be validated in the following cases. 1) Under drought stress, the significant and negative linear relationship of  $\Phi_{PSII}$ -PAR will weaken or even no longer hold true (see for example Fig. 7h). Thus, the estimations of the intercepts and slopes are unreliable to reflect the degree of drought stress. 2) When most observation points are obtained under low irradiance, the y-intercepts of the diurnal  $\Phi_{PSII}$ -PAR regressions under drought stress will still not decrease (see for example Fig. 7a). Therefore, there are some limitations in the application of the y-intercepts and slopes of the diurnal  $\Phi_{PSII}$ -PAR regressions to evaluate the degree of drought stress (Fig. A3).

The results show that drought stress led to a gradual transformation of the diurnal  $\Phi_{PSII}$ -PAR relationship from a significantly linear relationship to a nonlinear relationship. And the  $R^2$  of diurnal  $\Phi_{PSII}$ -PAR regression exhibited a strong linear correlation with SRWC (Fig. A3). This suggests that we can use the strength of the linearity of the  $\Phi_{PSII}$ -PAR relationship to evaluate the degree of drought (Fig. 7). Therefore, we propose to use the  $R^2$  of the diurnal  $\Phi_{PSII}$ -PAR regression as a drought stress indicator. The results for sea grass given by Durako (2012) also show that the  $R^2$  values of the  $\Phi_{PSII}$ -PAR regressions decreased under environmental stress. This indicates that the method proposed in this paper may be applicable to detect the stress of other types of vegetation. However, more studies on different type plants (especially C3 vegetation) are necessary to verify the applicability of this method.

## 5. Conclusions

In this study, we revealed that the linearity of the diurnal  $\Phi_{PSII}$ -PAR decreased under drought stress and proposed a more reliable indicator to detect drought stress on the leaf scale. Since  $\Phi_{PSII}$  and PAR can already be automatically observed in the field as a result of the development of observation technology (for example, Monitoring-PAM) (Porcar-Castell et al., 2008), the proposed method will make it possible to use chlorophyll fluorescence technology to automatically monitor crop drought stress in the field.

## 6. Data availability statement

The data that support the findings of this study are available on request from the corresponding author. The data are not publicly available due to privacy restrictions.

## CRediT authorship contribution statement

**Zhuang Chen:** Conceptualization, Methodology, Data curation, Validation, Formal analysis, Writing – original draft, Investigation, Writing – review & editing, Visualization. **Zhigang Liu:** Conceptualization, Writing – review & editing, Supervision, Project administration,

Funding acquisition. **Shuai Han:** Investigation. **Hao Jiang:** Investigation. **Shan Xu:** Investigation. **Huarong Zhao:** Investigation. **Sanxue Ren:** Investigation.

## Declaration of Competing Interest

The authors declare that they have no known competing financial interests or personal relationships that could have appeared to influence the work reported in this paper.

## Acknowledgements

We thank Peiqi Yang for comments and suggestions on this manuscript. This research was supported by the National Natural Science Foundation of China (grant no. 42071402) and the Water Resources Science and Technology Project of Jiangxi Province, China (202023ZDKT10, KT201706).

## Appendix

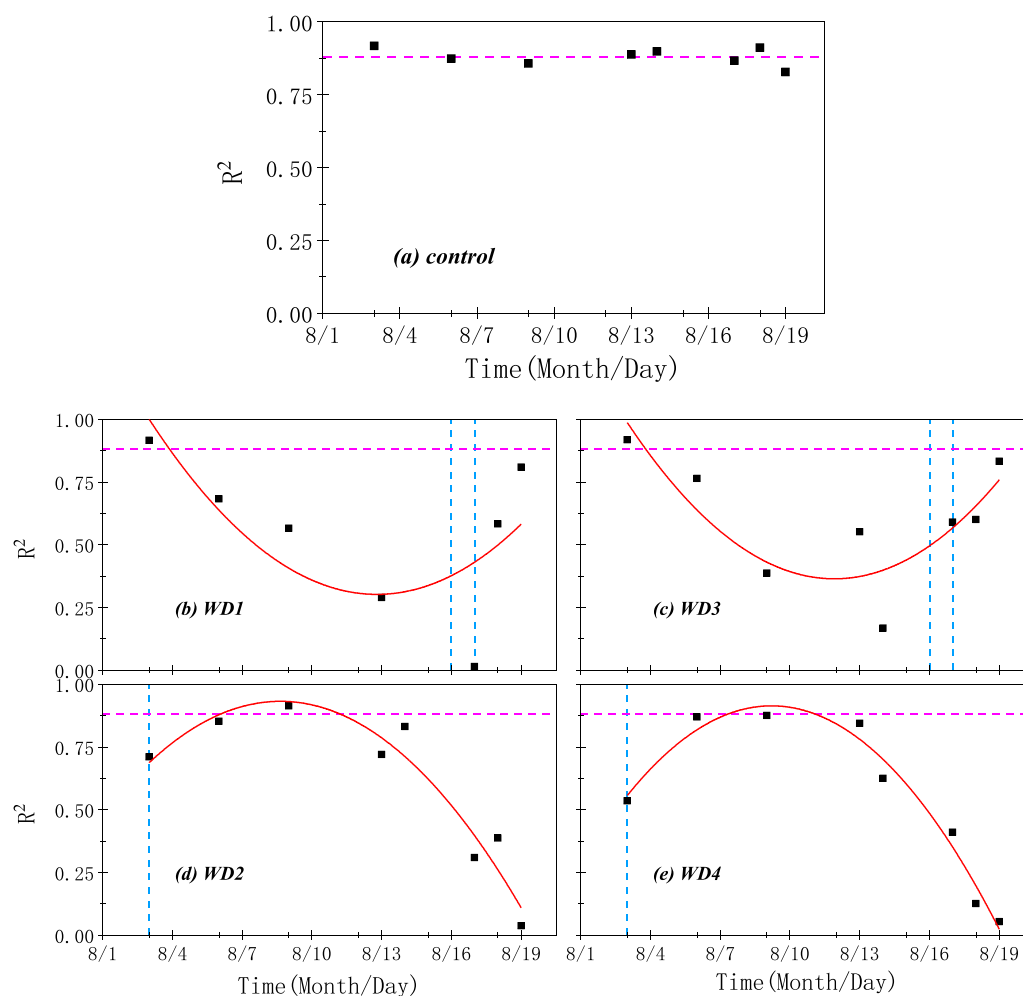


**Fig. A1.** Regression Coefficient between  $\Phi_{PSII}$  and PAR during August 3 to August 19 of control (a), WD1 (b), WD2 (c), WD3 (d), WD4 (e). The horizontal dotted line is the mean value of diurnal regression  $R^2$  of  $\Phi_{PSII}$  versus PAR in E-1 plot. The blue vertical dotted line indicates that the plot was rewatered that night. (For interpretation of the references to colour in this figure legend, the reader is referred to the web version of this article.)



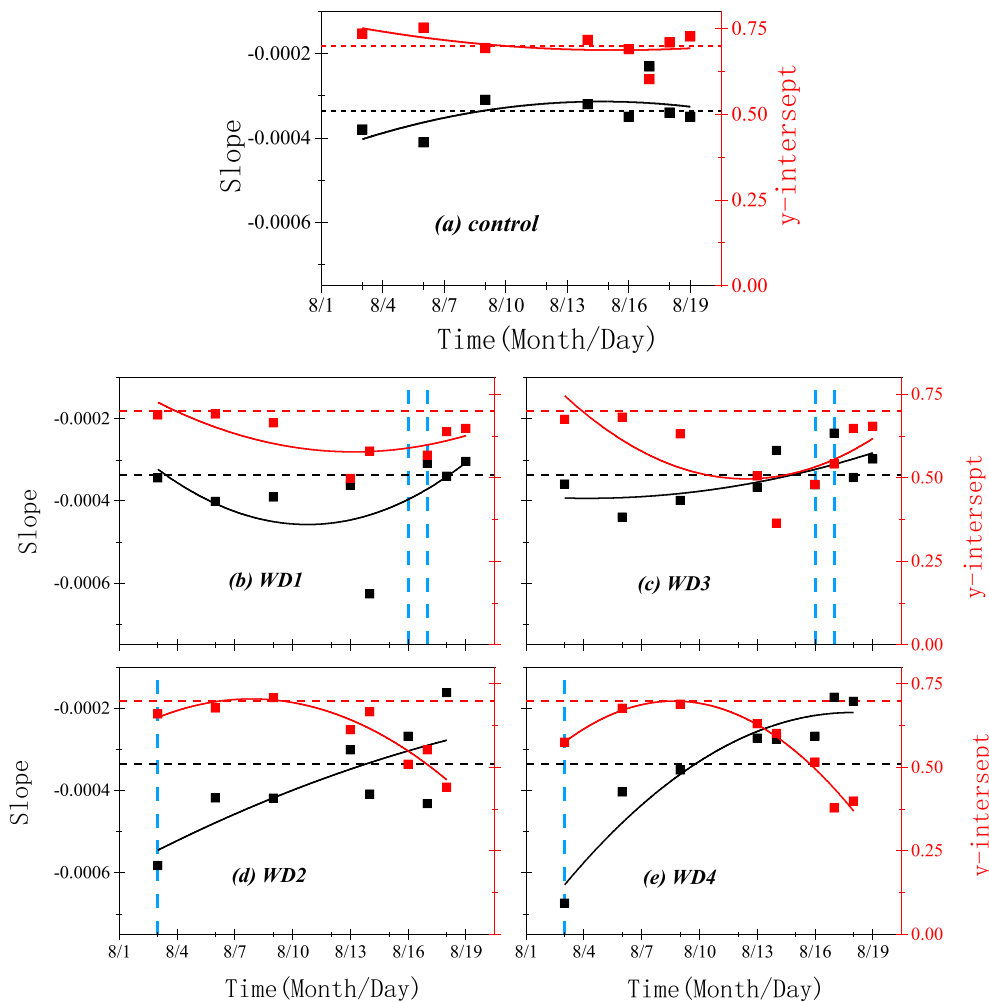


**Fig. A2.** The y-intercept (Red Triangle) and slope (Black Square) of diurnal  $\Phi_{PSII}$ -PAR relationship from August 3 to August 19 for (a) plot control, (b) plot WD1, (c) plot WD2, (d) plot WD3 and (e) plot WD4. The blue vertical dotted line indicates that the plot was rewatered that night. The horizontal red and black dotted lines are the mean value of diurnal regression y-intercept and slope of  $\Phi_{PSII}$  versus PAR in control plot respectively. (For interpretation of the references to colour in this figure legend, the reader is referred to the web version of this article.)

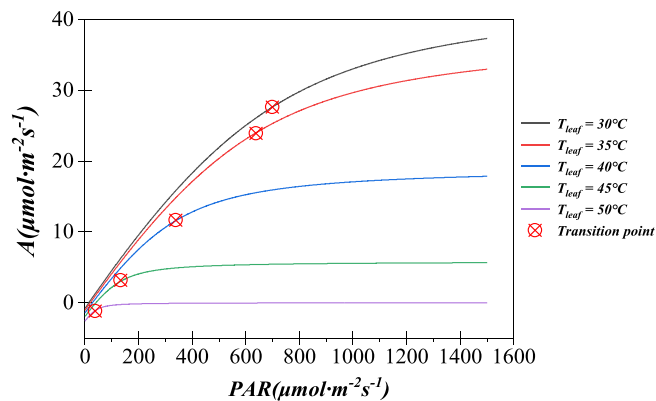


**Fig. A3.** The relationship between SRWC and the regression coefficients ( $R^2$ , y-intercept and slope) of diurnal  $\Phi_{PSII}$ -PAR. Red squares, blue dots, and black triangles represent  $R^2$ , y-intercept, and slope changes with SRWC, respectively.  $R^2_{\Phi_{PSII}-PAR}$  represents the  $R^2$  of diurnal  $\Phi_{PSII}$ -PAR regression. (For interpretation of the references to colour in this figure legend, the reader is referred to the web version of this article.)

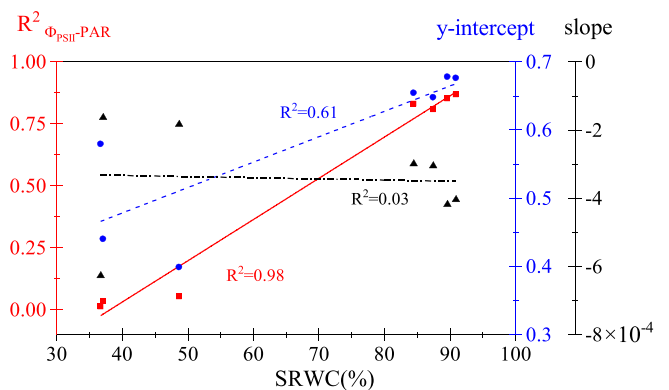


**Fig. A4.** A (net  $CO_2$  assimilation) changes with PAR at different  $T_{leaf}$  (30, 35, 40, 45, 50 °C) through the simulation of the biochemical modular in SCOPE model. The transition points between the light-limited state and the rubisco-limited state at each  $T_{leaf}$  level were marked in this plot.

## References

- Baker, N.R., 2008. Chlorophyll fluorescence: a probe of photosynthesis in vivo. *Annu. Rev. Plant Biol.* 59, 89–113.
- Baker, N.R., Rosenqvist, E., 2004. Applications of chlorophyll fluorescence can improve crop production strategies: an examination of future possibilities. *J. Exp. Bot.* 55, 1607–1621.
- Belshe, E., Durako, M.J., et al., 2007. Photosynthetic rapid light curves (RLC) of *Thalassia testudinum* exhibit diurnal variation. *J. Exp. Mar. Biol. Ecol.* 342, 253–268.
- Brestic, M., Zivcak, M., 2013. PSII fluorescence techniques for measurement of drought and high temperature stress signal in crop plants: protocols and applications. In: *Molecular stress physiology of plants*. Springer, pp. 87–131.
- Campbell, S., Miller, C., et al., 2003. Photosynthetic responses of two temperate seagrasses across a water quality gradient using chlorophyll fluorescence. *J. Exp. Mar. Biol. Ecol.* 291, 57–78.
- Collatz, G.J., Ball, J.T., et al., 1991. Physiological and environmental regulation of stomatal conductance, photosynthesis and transpiration: a model that includes a laminar boundary layer. *Agric. For. Meteorol.* 54, 107–136.
- Collatz, G.J., Ribas-Carbo, M., et al., 1992. Coupled photosynthesis-stomatal conductance model for leaves of C4 plants. *Funct. Plant Biol.* 19, 519–538.
- Datko, M., Zivcak, M., Brestic, M., 2008. Proteomic analysis of barley (*Hordeum vulgare* L.) leaves as affected by high temperature treatment. *Photosynthesis* 14.
- Demmig-Adams, B., Adams, W.W., 2018. An integrative approach to photoinhibition and photoprotection of photosynthesis. *Environ. Exp. Bot.* 154, 1–3.
- Durako, M.J., 2012. Using PAM fluorometry for landscape-level assessment of *Thalassia testudinum*: can diurnal variation in photochemical efficiency be used as an ecoindicator of seagrass health? *Ecol. Ind.* 18, 243–251.
- Flexas, J., Bota, J., et al., 2004. Diffusive and metabolic limitations to photosynthesis under drought and salinity in C3 plants. *Plant Biol.* 6, 269–279.
- Genty, B., Briantais, J., et al., 1989. The relationship between the quantum yield of photosynthetic electron transport and quenching of chlorophyll fluorescence. *Biochim. Biophys. Acta (BBA)-General Subjects* 990, 87–92.
- Ghannoum, O., 2009. C4 photosynthesis and water stress. *Ann. Bot.* 103, 635–644.
- Grassi, G., Vicinelli, E., Ponti, F., Cantoni, L., Magnani, F., 2005. Seasonal and interannual variability of photosynthetic capacity in relation to leaf nitrogen in a deciduous forest plantation in northern Italy. *Tree Physiol.* 25 (3), 349–360.
- Hazrati, S., Tahmasebi-Sarvestani, Z., et al., 2016. Effects of drought stress and light intensity on chlorophyll fluorescence parameters and pigments of *Aloe vera* L. *Plant Physiol. Biochem.* 106, 141–148.
- Howarth, J.F., Durako, M.J., 2013. Diurnal variation in chlorophyll fluorescence of *Thalassia testudinum* seedlings in response to controlled salinity and light conditions. *Mar. Biol.* 160, 591–605.
- Huang, W., Yang, S.-J., Zhang, S.-B., Zhang, J.-L., Cao, K.-F., 2012. Cyclic electron flow plays an important role in photoprotection for the resurrection plant *Paraboea rufescens* under drought stress. *Planta* 235 (4), 819–828.
- Koerber, G.R., Seekamp, J.V., et al., 2012. A putative hybrid of *Eucalyptus largiflorens* growing on salt-and drought-affected floodplains has reduced specific leaf area and leaf nitrogen. *Aust. J. Bot.* 60, 358–367.
- Lal, A., Edwards, G.E., 1996. Analysis of inhibition of photosynthesis under water stress in the C4 species *Amaranthus cruentus* and *Zea mays*: electron transport, CO2 fixation and carboxylation capacity. *Funct. Plant Biol.* 23 (4), 403–412.
- Lang, Y., Wang, M., et al., 2018. Effects of soil drought stress on photosynthetic gas exchange traits and chlorophyll fluorescence in *Forsythia suspensa*. *J. For. Res.* 29, 45–53.
- Li, Q.M., Liu, B.B., et al., 2008. Interactive effects of drought stresses and elevated CO2 concentration on photochemistry efficiency of cucumber seedlings. *J. Integr. Plant Biol.* 50, 1307–1317.
- Lichtenthaler, H.K., Rinderle, U., 1988. The role of chlorophyll fluorescence in the detection of stress conditions in plants. *CRC Crit. Rev. Anal. Chem.* 19 (sup1), S29–S85.
- Marshall, H.L., Geider, R.J., Flynn, K.J., 2000. A mechanistic model of photoinhibition. *New Phytol.* 145 (2), 347–359.
- Maxwell, K., Johnson, G.N., 2000. Chlorophyll fluorescence—a practical guide. *J. Exp. Bot.* 51 (345), 659–668.
- Müller, P., Li, X., et al., 2001. Non-photochemical quenching. A response to excess light energy. *Plant Physiol.* 125, 1558–1566.
- Murchie, E.H., Lawson, T., 2013. Chlorophyll fluorescence analysis: a guide to good practice and understanding some new applications. *J. Exp. Bot.* 64 (13), 3983–3998.
- O’Kelly, B.C., 2004. Accurate determination of moisture content of organic soils using the oven drying method. *Drying Technol.* 22, 1767–1776.
- Oliver, M.J., Cushman, J.C., et al., 2010. *Dehydration Tolerance in Plants*. Springer, Plant stress tolerance, pp. 3–24.
- O’Neill, P.M., Shanahan, J.F., et al., 2006. Use of chlorophyll fluorescence assessments to differentiate corn hybrid response to variable water conditions. *Crop Sci.* 46, 681–687.
- Pallas Jr, J., Michel, B.E., et al., 1967. Photosynthesis, transpiration, leaf temperature, and stomatal activity of cotton plants under varying water potentials. *Plant Physiol.* 42, 76–88.
- Pearcy, R.W., Yang, W., 1996. A three-dimensional crown architecture model for assessment of light capture and carbon gain by understory plants. *Oecologia* 108 (1), 1–12.
- Percival, G., 2005. The use of chlorophyll fluorescence to identify chemical and environmental stress in leaf tissue of three oak (*Quercus*) species. *J. Arboric.* 31 (5), 215–227.
- Porcar-Castell, A., Tyystjärvi, E., et al., 2014. Linking chlorophyll a fluorescence to photosynthesis for remote sensing applications: mechanisms and challenges. *J. Exp. Bot.* 65, 4065–4095.
- Porcar-Castell, A., Pfündel, E., Korhonen, J.F.J., Juurola, E., 2008. A new monitoring PAM fluorometer (MONI-PAM) to study the short-and long-term acclimation of photosystem II in field conditions. *Photosynth. Res.* 96 (2), 173–179.
- Salvatori, E., Fusaro, L., et al., 2014. Plant stress analysis: Application of prompt, delayed chlorophyll fluorescence and 820 nm modulated reflectance. Insights from independent experiments. *Plant Physiol. Biochem.* 85, 105–113.
- Schreiber, U., Schliwa, U., 1987. A solid-state, portable instrument for measurement of chlorophyll luminescence induction in plants. *Photosynth. Res.* 11, 173–182.
- Somerville, C., Briscoe, J., 2001. Genetic engineering and water. *Science* 292, 2217, 2217.
- Tombesi, S., Frioni, T., et al., 2018. Effect of drought stress “memory” on plant behavior during subsequent drought stress. *Environ. Exp. Bot.* 150, 106–114.
- Trenberth, K.E., Dai, A., et al., 2014. Global warming and changes in drought. *Nat. Clim. Change* 4, 17–22.
- Tribulato, A., Toscano, S., et al., 2019. Effects of drought stress on gas exchange, water relations and leaf structure in two ornamental shrubs in the Mediterranean area. *Agronomy* 9, 381.
- Van der Tol, C., Berry, J., et al., 2014. Models of fluorescence and photosynthesis for interpreting measurements of solar-induced chlorophyll fluorescence. *J. Geophys. Res. Biogeosci.* 119, 2312–2327.
- Van der Tol, C., Verhoef, W., et al., 2009. A model for chlorophyll fluorescence and photosynthesis at leaf scale. *Agric. For. Meteorol.* 149, 96–105.
- Vongcharoen, K., Santano, S., Banterng, P., Jogloy, S., Vorasoot, N., Theerakulpisut, P., 2019. Diurnal and seasonal variations in the photosynthetic performance and chlorophyll fluorescence of cassava ‘Rayong 9’ under irrigated and rainfed conditions. *Photosynthetica* 57 (1), 268–285.
- White, A.J., Critchley, C., 1999. Rapid light curves: a new fluorescence method to assess the state of the photosynthetic apparatus. *Photosynth. Res.* 59, 63–72.
- Yang, P., Prikaziuk, E., et al., 2021. SCOPE 2.0: A model to simulate vegetated land surface fluxes and satellite signals. *Geosci. Model Dev.* 14, 4697–4712.
- Zha, T.-S., Wu, Y.J., Jia, X., Zhang, M.Y., Bai, Y.J., Liu, P., Ma, J.Y., Bourque, C.-A., Peltola, H., 2017. Diurnal response of effective quantum yield of PSII photochemistry to irradiance as an indicator of photosynthetic acclimation to stressed environments revealed in a xerophytic species. *Ecol. Ind.* 74, 191–197.
- Zhao, L., Liu, Z., Xu, S., He, X., Ni, Z., Zhao, H., Ren, S., 2018. Retrieving the diurnal FPAR of a maize canopy from the jointing stage to the tasseling stage with vegetation indices under different water stresses and light conditions. *Sensors* 18 (11), 3965.